crystals

MDPI

Article

Insight into the Structural, Mechanical and Optoelectronic Properties of Ternary Cubic Barium-Based $BaMCl_3$ (M = Ag, Cu) Chloroperovskites Compounds

Mudasser Husain [1,*], Abd Ullah [2], Ali Algahtani [3,4], Vineet Tirth [3,4], Tawfiq Al-Mughanam [5,*], Abdulaziz H. Alghtani [6], Nourreddine Sfina [7,8,*], Khaoula Briki [9], Hind Albalawi [10], Mohammed A. Amin [11], Ahmed Azzouz-Rached [12] and Nasir Rahman [1,*]

1 Department of Physics, University of Lakki Marwat, Lakki Marwat 28420, Pakistan
2 Department of Physics, Kohat University of Science and Technology, Kohat 26000, Pakistan
3 Mechanical Engineering Department, College of Engineering, King Khalid University, Abha 61421, Saudi Arabia
4 Research Center for Advanced Materials Science (RCAMS), King Khalid University, Guraiger, P.O. Box 9004, Abha 61413, Saudi Arabia
5 Department of Mechanical Engineering, College of Engineering, King Faisal University, P.O. Box 380, Al-Ahsa 31982, Saudi Arabia
6 Department of Mechanical Engineering, College of Engineering, Taif University, P.O. Box 11099, Taif 21944, Saudi Arabia
7 College of Sciences and Arts in Mahayel Asir, Department of Physics, King Khalid University, Abha 62217, Saudi Arabia
8 Laboratoire de la Matière Condensée et des Nanosciences (LMCN), Département de Physique, Faculté des Sciences de Monastir, Université de Monastir, Avenue de l'Environnement, Monastir 5019, Tunisia
9 College of Sciences for Girls-Dammam, Imam Abdulrahman Bin Faisal University, P.O. Box 1982, Dammam 31441, Saudi Arabia
10 Department of Physics, College of Sciences, Princess Nourah Bint Abdulrahman University (PNU), P.O. Box 84428, Riyadh 11671, Saudi Arabia
11 Department of Chemistry, College of Science, Taif University, P.O. Box 11099, Taif 21944, Saudi Arabia
12 Magnetic Materials Laboratory, Faculty of Exact Sciences, Djillali Liabes University of Sidi Bel-Abbes, Sidi Bel Abbès 22000, Algeria
* Correspondence: mudasserhusain01@gmail.com (M.H.); talmughanam@kfu.edu.sa (T.A.-M.); nsfina@kku.edu.sa (N.S.); nasir@ulm.edu.pk (N.R.)

Abstract: Prediction of new materials is crucial for the advancement of technology. Here, in this research work, the first-principle computation has been conducted utilizing the WIEN2K package to probe the structural, electronic, mechanical, and optical properties of barium-based chloroperovskites $BaMCl_3$ (M = Ag, Cu) compounds. The optimized lattice constants are calculated for both compounds which are 9.90 Bohr for $BaAgCl_3$ and 9.38 Bohr for $BaCuCl_3$. To obtain better and more precise results for the electronic band's structure, TDOS and PDOS (total and partial density of states), and the TB-mBJ potential approximation are employed. The indirect band gap (R–Γ) is found for both compounds having values of 1.173 eV and 2.30 eV for $BaCuCl_3$ and $BaAgCl_3$, respectively, which depicts its semiconducting nature. The calculation of elastic properties is conducted with IRelast code. The Cauchy pressure, Bulk modulus, Young's modulus, Shear modulus, anisotropic ratio, Kleinman parameters, and Poisson's ratio are calculated from the obtained elastic constants. The computation of elastic parameters indicates that the interested chloroperovskites are anisotropic, mechanically stable, hard to scratch, and ductile. From 0 eV to 40 eV incident photon energy ranges, the various optical parameter such as refractive index, absorption coefficient, dielectric function, reflectivity, extinction coefficient, and optical conductivity are analyzed. These compounds absorb maximum light within 5 to 25 eV incident photon energy. Hence, these materials are good light absorbers, therefore, they can be used in optoelectronic devices for high-frequency applications.

check for updates

Citation: Husain, M.; Ullah, A.; Algahtani, A.; Tirth, V.; Al-Mughanam, T.; Alghtani, A.H.; Sfina, N.; Briki, K.; Albalawi, H.; Amin, M.A.; et al. Insight into the Structural, Mechanical and Optoelectronic Properties of Ternary Cubic Barium-Based $BaMCl_3$ (M = Ag, Cu) Chloroperovskites Compounds. *Crystals* **2023**, *13*, 140. https://doi.org/10.3390/cryst13010140

Academic Editors: Zeng Liu and Shan Li

Received: 27 November 2022
Revised: 8 January 2023
Accepted: 9 January 2023
Published: 13 January 2023

Keywords: WIEN2K; DFT; chloroperovskites; structural properties; optoelectronic properties; mechanical properties

1. Introduction

As the population of the world is growing drastically, the energy crises are catching increasing day by day. It proves the importance of energy in the field of economic growth and a higher standard of living [1]. The careless usage of energy creates a gap between the required and supply of energy, which ultimately affects nearly all economic fields. To overcome the energy gap, human beings need cheaper and environmentally friendly renewable energy sources [2]; among these sources, solar energy is the most economical and eco-friendly [3]. We can use solar energy directly (heating and warming objects) and indirectly (converting it to electrical energy by using certain devices). The device (solar cell) is primarily based on the rule of activation of electrons through solar light creating electron-hole pairs, ultimately giving the electricity [4]. In the past, solar cells were mostly fabricated from Si-based materials. However, at present, the researcher is working on Perovskite-based solar cells to enhance power-converting efficiency and minimize power loss [5,6]. In 1839 Gustav Rose, a German scientist, discovered $CaTiO_3$, a new kind of material exhibiting the structure ABX_3 in the Ural mountain region; it was named after Lev von Perovski (Russian mineralogist) as "Perovskites" [7]. Perovskite materials are attracting the researcher's attention because of their versatile structure and distinctive electromagnetic, elastic, thermal, optical, and electronic behaviour [8,9]. The hybrid halide $CH_3NH_3PbBr_3$ and $CH_3NH_3PbI_3$ perovskite materials were first used in 2009 in the dye-sensitized solar cells industry, delivering excellent power conversion efficiency [10]. Currently, $CsRhCl_3$ and $CsBeCl_3$ are being studied by Umar Ayaz Khan et al. [11], who described that both materials are mechanically and structurally stable and a paramagnetic, and ductile nature is recorded for these materials. $ASnO_3$ (A = Sr, Ca, and Ba) was investigated by Djellal Cherrad et al. [12] who noted the indirect band gap (R–G) confirming their semiconducting nature and proposed that these compounds can be excellent materials for shielding devices in ultra-violet radiations range because of its high reflectivity. Kashif Murad et al. predicted some physical properties in their work that both $BaAgCl_3$ and $BaCuCl_3$ ternary chloroperovskites compounds are stable [13]. Their work is limited to predicting the stability and some physical properties. The stability of these chloroperovskites materials is also reported by Gómez-Peralta et al. [14]. We have computed precisely and accurately the structural, phonons dynamical stability, elastic, electronic, and optical properties of the selected ternary chloroperovskites compounds and we are assured of our outcomes. Our investigations will provide a pathway for the experimentalist to verify it experimentally. These $BaMCl_3$ (M = Ag, Cu) compounds are interesting materials for the applications of optoelectronics and many modern technologies. Here, we explored the diverse properties such as the structural, phonon dynamical stability, electronic, optical, and elastic properties of $BaXCl_3$ (M = Ag, Cu) through DFT within the WIEN2K package (WIEN2K 18.02, Creater Peter Blaha, Vienna Austria). Structural properties of both the materials are carried out from the optimization curve bulk modulus and tolerance factor, while the electronic properties are explored from band gap and DOS. The elastic properties are computed from the elastic constant. The refractive index, reflectivity, absorption coefficient, optical conductivity, and extinction coefficient, are studied for optical properties.

2. Computational Methodologies

The first-principle computations perform precise investigations and are increasingly capable of calculating material properties at the atomic/electronic level. This research is conducted using the DFT approach executed within the WIEN2K simulation code [15]. The volume of the unit cell is disintegrated into two portions: (1) The sphere of non-intersecting muffin-tin radius (RMT) centered at the nuclear positions and (2) the interstitial sphere. The

electronic density and the exchange-correlation potential are extended into combinations of spherical harmonics time's radial functions within the MT spheres and Fourier expansions in the interstitial position. The values of RMT are picked for constituent atoms so that there is no overlapping within the RMT. The RMTs values for the constituent atoms are 2.5, 1.78, and 1.92 atomic units for "Ba", and "M" where (M = Ag and Cu), and "Cl", respectively. The determination of the electronic structure of solid crystal density functional theory (DFT) approach has proved itself to be one of the most efficient techniques [16,17]. Here, the full-potential linearized augmented plane wave (FP-LAPW) approach [18] inside the frame of DFT is used to compute the electronic and optical structure. Kohn-sham's equations are consistently solved for obtaining the total energies within TB-mBJ approximation [19–21]. The structural parameters are computed by fitting the unit cell volume vs. unit cell energy through the Birch–Murnaghan equation of state [22]. The TB-mBJ potential approximation is applied to calculate the electronic properties of both compounds [23]. Elastic constants are obtained through the IRelast package from which the diverse mechanical parameters are investigated. From $\varepsilon(\omega) = \varepsilon_1(\omega) + i\varepsilon_2(\omega)$ (complex dielectric function), we have determined the optical character of both compounds in which $\varepsilon_1(\omega)$ shows the real and $\varepsilon_2(\omega)$ represent an imaginary part. The $\varepsilon_2(\omega)$ was computed from the momentum matrix of unoccupied and occupied wave functions, while the $\varepsilon_1(\omega)$ is achieved from $\varepsilon_2(\omega)$ through Kramers–Kronig relations [24,25]. The expression of the lattice harmonics angular momentum cuts at l_{max} = 10 and up to G_{max} = 14 Bohr^{-1}, the Fourier expansion runs, while the wave function in the interstitial regions is described by plane wave expansions. The cut-off value of K_{max} displays the determined number of plane waves and depends on the parameter of $R_{MT} \times K_{max}$ = 6.5 (in these investigations) and 2000 k-points are taken to obtain the precise result.

3. Structural Properties

Herein, the investigated compounds $BaMCl_3$ (M = Ag, Cu) crystallize into the ideal cubic structure of perovskite having space group (#221). The unit cell contains one molecule of $BaMCl_3$. The constituent atom lies at positions (0, 0, 0), (0.5, 0.5, 0.5), and (0, 0.5, 0.5) for Ba, M, and Cl, respectively. The crystal structures are displayed in Figure 1.

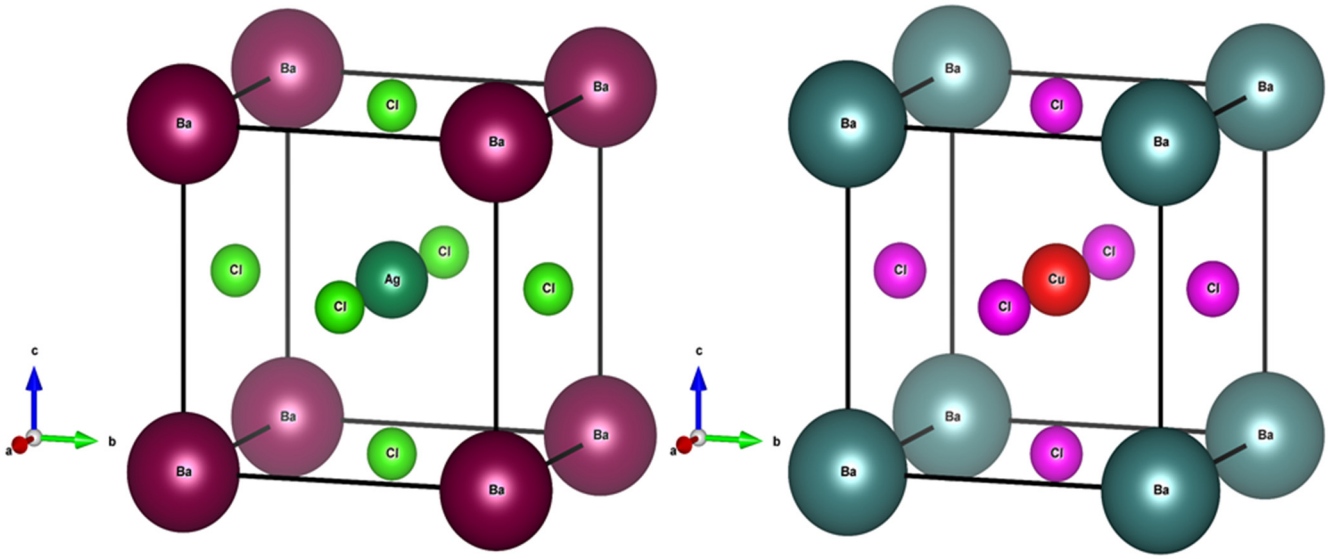

Figure 1. The crystal structures of $BaMCl_3$ (M = Ag, Cu) compounds.

To measure the thermodynamic stability and synthesizability, the enthalpy of formation is computed through formulas:

$$H = E + PV \quad (1)$$

For both compounds, the "H" values are negative. The negative values of enthalpy for both compounds signify the thermodynamic stability and the formation of the interested compound [26]. Furthermore, to investigate the structural stability, the Goldschmidt tolerance factor is computed from the ionic radii [27]. By using the volume optimization graph, the lattice parameters are computed at minimum energy and the calculated values are present in Table 1. The optimized volume versus energy curve is plotted in Figure 2. Table 1 clarifies that with an increase in the lattice constant, the bulk modulus decreases indicating the hardness of $BaAgCl_3$ is more than $BaCuCl_3$.

Table 1. The optimized crystal structural parameters comprising lattice constant (in Bohr), Bulk modulus (in GPa), ground state volume in $(Bohr)^3$, $B^{/}$ (the derivative of Bulk modulus in GPa), ground state energy E_0 in Ry and the tolerance factor τ.

Structural Parameters	$BaAgCl_3$	$BaCuCl_3$
Lattice constant (Bohr)	9.90	9.38
Bulk modulus (B)	34.19	43.03
Ground state volume (V_0)	968.2	820.78
Bulk modulus derivative ($B^{/}$)	5.52	7.66
Ground state energy (E_0)	−29,682.92	−22,358.39
Tolerance factor (τ)	0.93	0.97

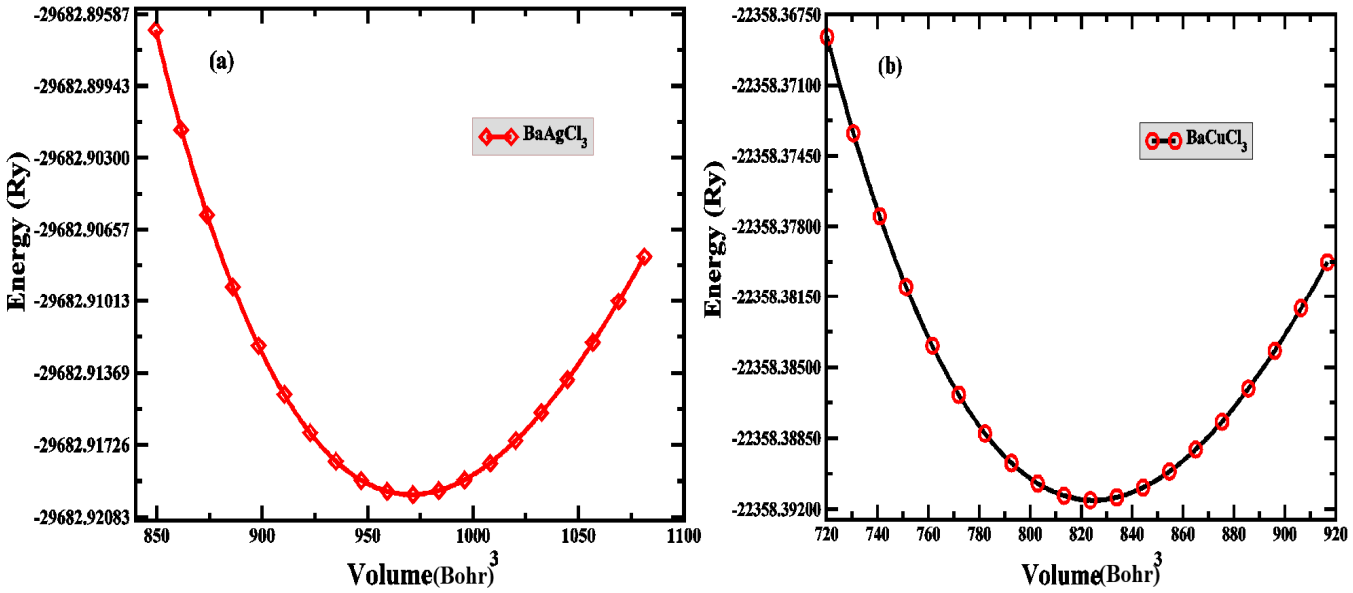

Figure 2. Illustration of volume optimization curves for (**a**) $BaAgCl_3$ and (**b**) $BaCuCl_3$.

From the above presented optimized structural parameters, it is concluded that both the materials $BaMCl_3$ (M = Ag, and Cu) are structurally stable and optimized.

Phonon Properties

Phonons are a crucial component of dynamic behaviors and thermal characteristics, which are the main aspects of the fundamental problems of materials science. The phonon dispersion band structure of cubic ternary $BaAgCl_3$ and $BaCuCl_3$ are investigated using the WIEN2K package within the frequency range from 0 THz up to 16 THz, as depicted in Figure 3. It can be seen from Figure 3 that the phonon dispersion curves for both materials are positive and there are no negative values of dispersion curves (imaginary phonon frequencies). The positive dispersion curves confirm the phonon dynamical stability of both compounds.

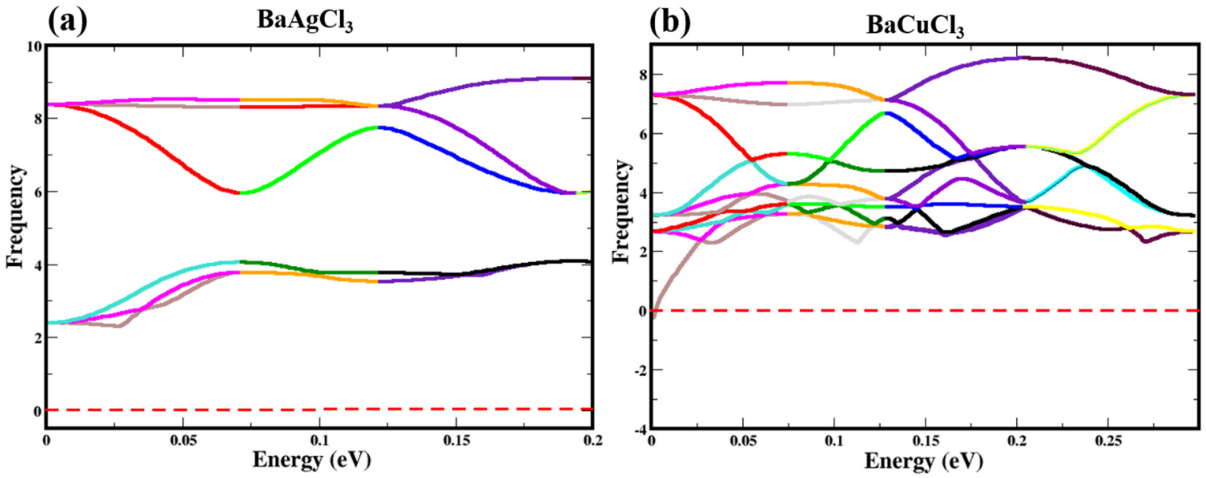

Figure 3. The computed phonon dispersion bands structure of cubic ternary (**a**) $BaAgCl_3$ and (**b**) $BaCuCl_3$ chloroperovskites compounds.

4. Electronic Properties

The fitted band structures and densities of states (DOS) within the energy range from −8 eV to 8 eV are conducted for the computation of electronic properties of $BaAgCl_3$ and $BaCuCl_3$ ternary chloroperovskites. The TB-mBJ approximation is applied to investigate the band structures of both ternary $BaAgCl_3$ and $BaCuCl_3$ chloroperovskites compounds, shown in Figure 4. The Fermi energy level (E_F) separates the valence and conduction states. Valance band maxima and conduction band minima appear at the different symmetry points, i.e., from R–Γ, and hence, possess the indirect band gap with values 1.173 eV and 2.30 eV for $BaCuCl_3$ and $BaAgCl_3$, respectively. The $BaAgCl_3$ possesses a higher band gap than $BaCuCl_3$ due to the high electronegativity of Ag than Cu.

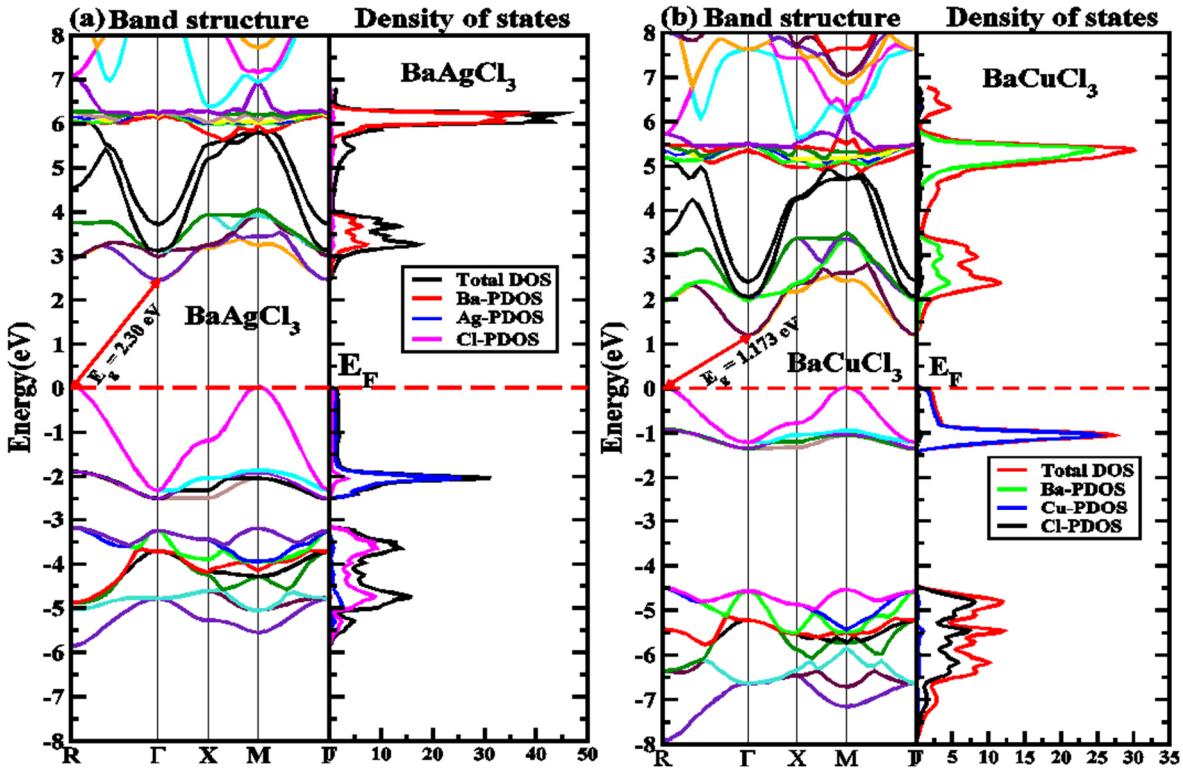

Figure 4. The electronic band structures of (**a**) $BaAgCl_3$ and (**b**) $BaCuCl_3$.

TDOS and PDOS for $BaCuCl_3$ and $BaAgCl_3$ are plotted in Figure 5a,b, respectively, to analyze the impact of different electronic states in valence and conduction bands. Figure 5a clarifies that the valance band of $BaCuCl_3$ consists of Cl p-orbital from −4.5 to −8 eV have high contribution and p, d-orbital from −1.5 to 0 eV energy have little contribution and Cu d-orbital contribute from energy 0 to −2 eV, while Ba has no contribution to the valance band. In the conduction band, Ba-d and f orbitals from 2 to 6 eV, Cu s-p orbital contribute in the range of 4 up to 6 eV, while s, p, d-orbitals of "Cl" contribute from 2 up to 8 eV. Figure 5b clarifies that the valance band of $BaAgCl_3$ mainly consists of Cl-p, and Ag-d orbital from 0 to −6 eV, while "Ba" has no contribution to the valance band. In the conduction band Ag-s, Ba-d, f, and p, d-orbitals of Cl mainly contribute from energy 2 up to 6 eV. The band structures and DOS indicate the existence of a band gap between the conduction and valance bands in both compounds justifying that these compounds are semiconductors in nature.

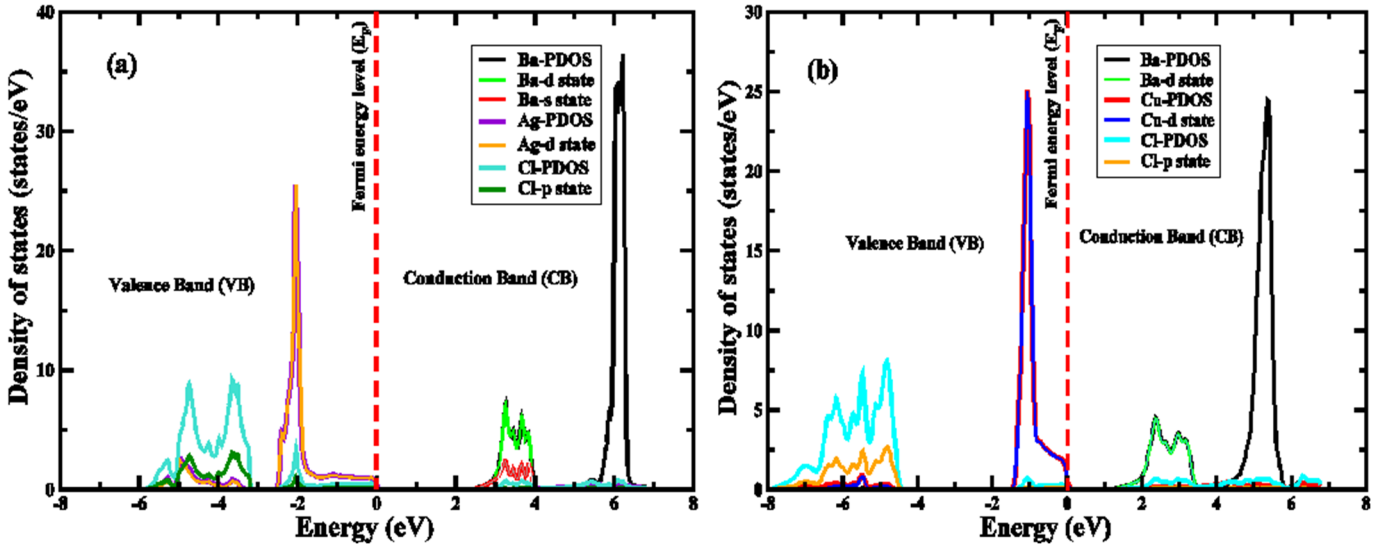

Figure 5. The TDOS and PDOS of (**a**) $BaAgCl_3$ and (**b**) $BaCucCl_3$.

5. Elastic Properties

The mechanical properties of a material are interrelated to essential solid-state phenomena including inter-atomic bonding, phonon spectra, and equation of state that play a vital role in structural stability and resistance to external forces. Many mechanical properties such as fracture toughness, ductility, brittleness, thermo-elastic stress, sound velocities, internal strain, etc., can be explained through elastics constants [28–30]. Herein, the elastic constants are investigated through the IRelast package developed by J. Murtaza [31]. As both compounds are FCC, the elastics constants C_{11}, C_{12}, and C_{44} are sufficient to explain their elastics characteristics. The investigated elastics constants C_{11}, C_{12}, and C_{44} are present in Table 2.

Table 2. The computed elastic parameters including the cubic elastic constants (C_{11}, C_{12}, and C_{44} in GPa), the Bulk modulus "B" (in GPa), anisotropy factor "A", Shear modulus "G" (in GPa), Young's modulus "E" (in GPa), Poisons ration "υ" and the Pugh ratio (B/G) and the Kleinman parameter (ζ).

Compounds	C_{11}	C_{12}	C_{44}	B	A	G	E	υ	B/G	ζ
$BaAgCl_3$	89.42	25.31	3.35	46.68	0.10	4.80	13.9	0.66	9.73	0.793
$BaCuCl_3$	105.16	40.6	19.93	62.12	0.61	15	2.00	0.74	4.14	0.878

For structure stability, the elastics constants should satisfy the Born stability criteria which are

$$C_{11} - C_{12} > 0, C_{44} > 0, C_{11} + 2C_{12} > 0 \quad (2)$$

Based on our calculated elastics constant we can conclude that both compounds are structurally stable and resist elastic deformation [32]. Bulk modulus, Young's modulus, Shear modulus, anisotropic ratio, Poisson's ratio, and Kleinman parameters are other essential mechanical properties of solids for industrial applications. Table 2 clarifies that the value of bulk modulus "B" is higher for $BaAgCl_3$ than $BaCuCl_3$, showing that $BaCuCl_3$ is more compressible than $BaAgcl_3$ when they are compressed from all sides. The value of "B" depends upon the lattice constant of the compound, and similarly, the bulk modulus and volume are inversely proportional to each other. Our calculated result is in agreement with this literature [20,21]. Cauchy pressure ($C_{12} - C_{44}$), Poisson's ratio, and Pugh ratio predict the brittle (ductile) nature of the material. If the value of Cauchy's pressure is negative (positive) the material will be brittle (ductile). For the investigated compounds the value is positive hence both are ductile. Pugh's criteria suggest that material will be brittle if the B/G value is smaller than 1.75 and ductile for the value of B/G is greater than 1.75 [33,34]. For a Poisson's ratio greater (smaller) than 0.26, the material will be ductile (brittle). From Table 2, the Pugh's ratio and Poisson ratio is greater than 1.75 and 0.26 for $BaAgCl_3$ than $BaCuCl_3$, respectively, hence both compounds are ductile [35]. Cauchy's pressure also defines the bonding nature of the material. For the ionic nature of the material, the material will have a positive value of Cauchy's pressure and a negative for covalent bonding [36,37]. The anisotropic ratio (A) is applied to determine the degree of elastic anisotropy in a solid material. An ideal isotropic system has an anisotropic ratio of one. When the value is "A" rather than unity, the material is said to be elastically anisotropic, meaning its elastic characteristics vary in different directions. The calculated value of "A" is not equal to "1" which is presented in Table 2, hence the compounds are anisotropic [38]. Another important parameter that describes bond stretching and bond bending is the Kleinman parameter (ζ). The zero value of the Kleinman parameter (ζ) indicates the minimum bond bending and when its value is 1, it shows minimum bond stretching. Table 2 clarifies that the value of ζ for $BaCuCl_3$ is 0.878 and that for $BaAgCl_3$ is 0.793, reflecting that the bond stretching of the selected compound is minimal [37,39].

6. Optical Properties

Herein, the parameters in optical properties are explored which include the dielectric function, optical conductivity, reflectivity, absorption coefficient, and refractive index of halide perovskite in the energy range from 0 to 40 eV. The complex dielectric function described the optical properties of the material. According to Ehrenreich and Cohen's equation [40], the dielectric can be written as:

$$\varepsilon(\boldsymbol{\omega}) = \varepsilon_1(\boldsymbol{\omega}) + \boldsymbol{i}\varepsilon_2(\boldsymbol{\omega}) \quad (3)$$

Here, the $\varepsilon_1(\boldsymbol{\omega})$ displays the real part and $\varepsilon_2(\boldsymbol{\omega})$ shows an imaginary component of the dielectric function and they can be determined from the following equations [25,41]:

$$\varepsilon_1(\omega) = 1 + \frac{2}{\pi} P \int_0^{\infty} \frac{\omega' \varepsilon_2(\omega')}{\omega'^2 - \omega^2} \, d\omega' \quad (4)$$

$$\varepsilon_2(\omega) = \frac{8}{2\pi\omega^2} \sum_{nn'} \int |p_{nn'}(k)|^2 \frac{dS_k}{\nabla \omega_{nn'}(ks)} \quad (5)$$

The dispersive behavior of compounds can be determined from the real component of the dielectric function whereas, the imaginary component gives information about the absorption of light [42,43]. Other optical parameters such as absorption coefficient, refractive index, optical conductivity, extension coefficient, and reflectivity can be described from the real and imaginary parts of the dielectric function. Figure 6a depicts the real

part of the function and the values of $\varepsilon_1(\omega)$ at zero frequency are 3.8 and 4.48 for $BaAgcl_3$ and $BaCuCl_3$, respectively. The greater value of $BaCuCl_3$ indicates a smaller band gap as compared to $BaAgCl_3$. The maximum peaks of the real part approach 6.79 at 4.50 eV for $BaAgCl_3$ and 6.009 at 5.8 eV for $BaCuCl_3$. The minima of the real part are about the same at 18.1 ev of value −2.1, indicating its metallic behavior. The obtained curved for the imagery part of the function is plotted in Figure 6b.

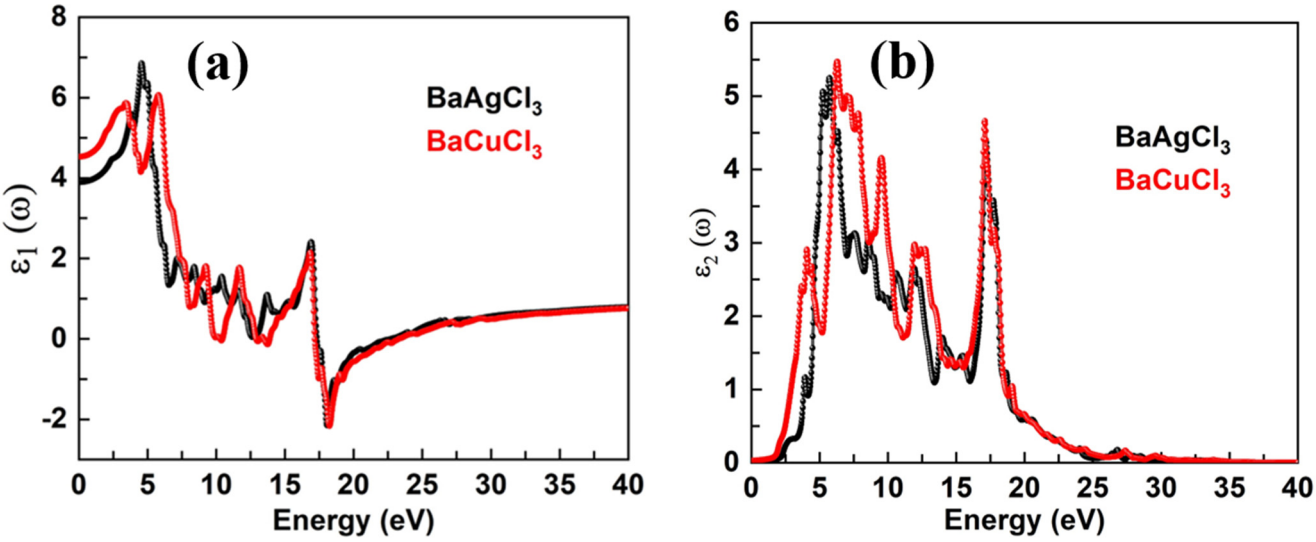

Figure 6. The Complex dielectric functions of (**a**) $BaAgCl_3$ and (**b**) $BaCucCl_3$.

It can be observed that the peak starts from 2.1 and 2.3 for $BaAgCl_3$ and $BaCuCl_3$, respectively, which means that the photon absorption starts from this energy range and the photons having less energy than these values are not able to be used for the transition of electrons from the valance to the conduction band. Moreover, the maximum peak reached 5.23 at 5.79 eV and 5.4 at 6.4 eV for $BaAgCl_3$ and $BaCuCl_3$, respectively. The indirect band gap and band-to-band transition are confirmed by the fluctuating peaks.

6.1. Extension Coefficient and Refractive Index

Utilizing the following expression the extension coefficient and refractive index are calculated.

$$k(\omega) = \left[\frac{\sqrt{\varepsilon_1{}^2(\omega) + \varepsilon_2{}^2(\omega)}}{2} - \frac{\varepsilon_1(\omega)}{2}\right]^{1/2} \quad (6)$$

$$\boldsymbol{n}\,(\omega) = \left[\frac{\sqrt{\varepsilon_1{}^2(\omega) + \varepsilon_2{}^2(\omega)}}{2} + \frac{\varepsilon_1(\omega)}{2}\right]^{1/2} \quad (7)$$

On the bases of the refractive index of the material, one can judge its application in optical devices. Materials having a high refractive index can be used in a photovoltaic cell. In Figure 7 the refractive index and extension coefficient are plotted. From Figure 7, it is noted that the value of (0) is 1.96 and 2.12 for $BaAgCl_3$ and $BaCuCl_3$, respectively.

The maximum values of n(0) for $BaAgCl_3$ and $BaCuCl_3$ are 2.63 at 4.64 eV, and 2.56 at 5.98 eV, respectively. The photon and electrons of compounds will interact with each other and after an interaction; the photon will slow down because of a refractive index value greater than 1.

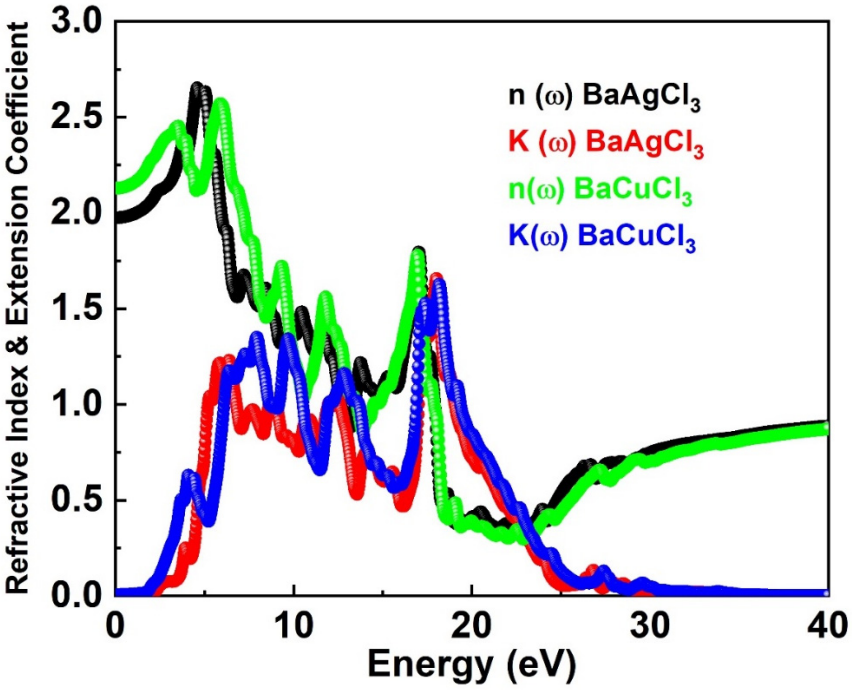

Figure 7. The refractive index and extension coefficient of ternary $BaAgCl_3$ and $BaCuCl_3$ chloroperovskites compounds.

6.2. Reflectivity

The numerical value of reflectivity R(ω) can be calculated from the refractive index and extension coefficient through the following expression:

$$R(\omega) = \frac{(1-n)^2 + k^2}{(1+n)^2 + k^2} \tag{8}$$

The obtained spectra for reflectivity are plotted in Figure 8.

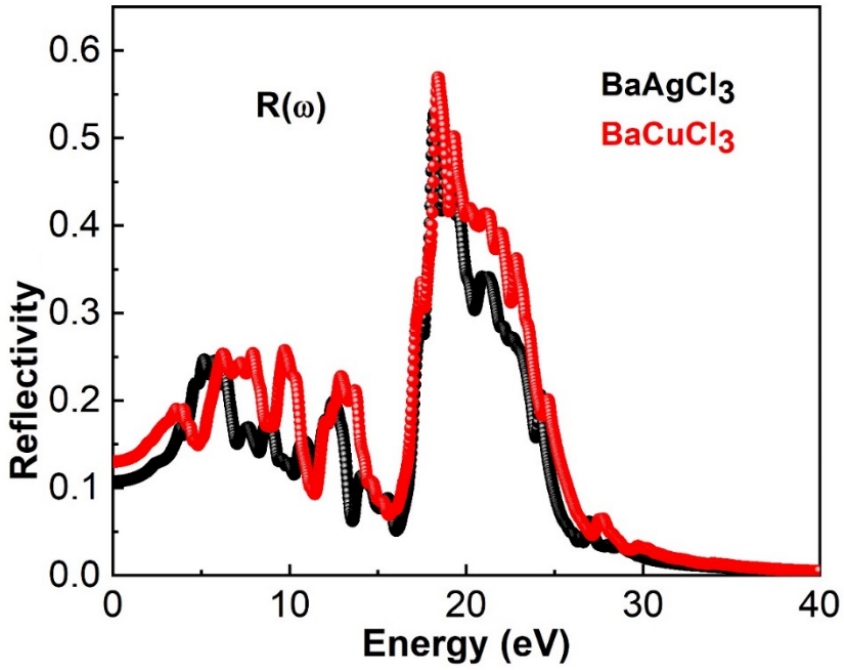

Figure 8. The optical reflectivity of ternary $BaAgCl_3$ and $BaCuCl_3$ chloroperovskites compounds.

The value of reflectivity at zero energy is 0.106 and 0.12 for $BaAgCl_3$ and $BaCuCl_3$, respectively. The materials are more reflective in the energy range of 16 eV to 25 eV. The highest peak is found at 0.524 at 18.17 eV for $BaAgCl_3$ while for $BaCuCl_3$ the highest peak is 0.566 at 18.4 eV.

6.3. Absorption Coefficient

A material's ability to transmit light of a specific wavelength for a certain distance before it is absorbed depends on its absorption coefficient. Using the following expression, the I (ω) can be determined:

$$I(\omega) = \frac{4\pi k}{\lambda} \tag{9}$$

Whereas, λ and k are the wavelength and extinction coefficient. The absorption coefficient shows the absorption of photons per unit length by material. The absorbed photon transmits the electron from the valance to the conduction band by giving them suitable energy. The spectra of the absorption coefficient are shown in Figure 9. From Figure 9 it is noted that this material absorbs energy in the range of 5 to 25 eV.

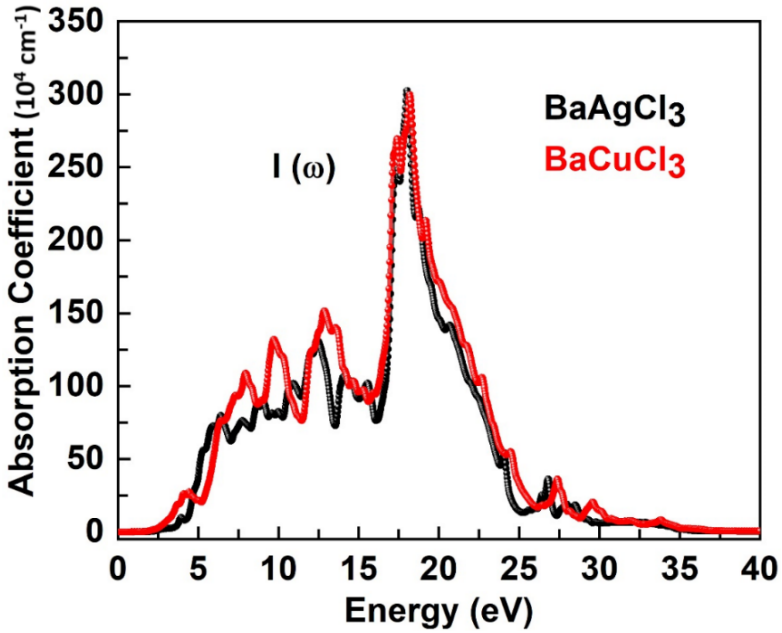

Figure 9. The absorption coefficient of ternary $BaAgCl_3$ and $BaCuCl_3$ chloroperovskites compounds.

Hence, these materials are good light absorbers; therefore, they can be used in optoelectronic devices. From the absorption coefficient spectra, it can also be observed that $BaCuCl_3$ is a good absorber as compared to $BaAgCl_3$. The highest peak is found for $BaCuCl_3$ to be 296 at 18.3 eV while for $BaAgCl_3$ it is noted at 300 at 18.17 eV.

6.4. Optical Conductivity

By using the following expression we can calculate the optical conductivity

$$\sigma(\omega) = \frac{2\,\hbar\omega}{E_0} \tag{10}$$

Whereas, "ω" is the incident frequency of the photon and E_0 is the photon energy. The obtained spectra for optical conductivity are presented in Figure 10, indicating that $BaCuCl_3$ is more optical conductive as compared to $BaAgCl_3$.

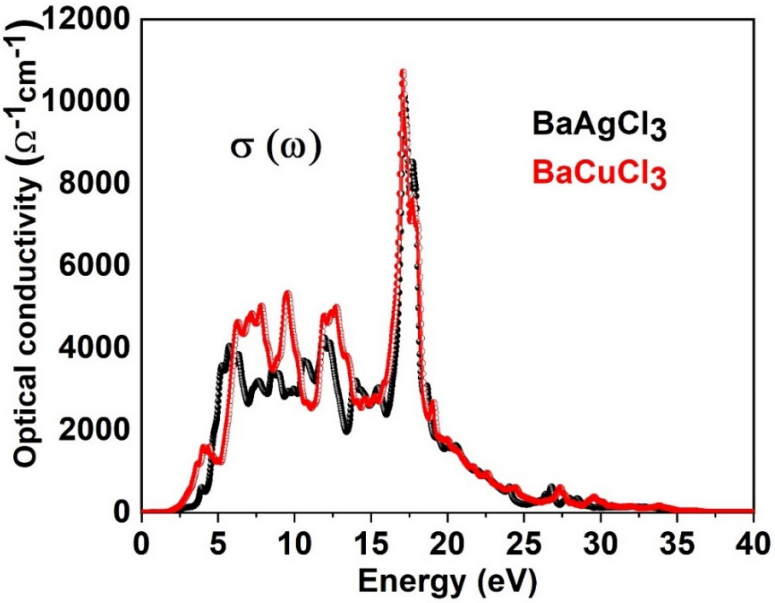

Figure 10. The optical conductivity of ternary $BaAgCl_3$ and $BaCuCl_3$ chloroperovskites compounds.

The maximum value of optical conductivity is found at 10,200 at 17.25 eV and 10,700 at 17.13 eV, respectively. The materials show conductance in the 5 eV to 20 eV energy range.

7. Conclusions

The structural, electronic, mechanical, and optical properties of $BaAgCl_3$ and $BaCuCl_3$ are explored for the first time through density functional theory. The structural properties reveal that $BaAgCl_3$ and $BaCuCl_3$ have stable structures and the negative enthalpy conforms to their formation. The electronic structure shows its semi-conducting nature with an indirect band gap (R–Γ) of value 1.173 eV and 2.30 eV for $BaCuCl_3$ and $BaAgCl_3$, respectively. It is found that $BaCuCl_3$ is more compressible than $BaAgCl_3$. Furthermore, the study of elastic properties reveals that both compounds are ductile, anisotropic, and possess an ionic bonding nature. Various spectrums of optical parameters are studied and from the optical spectrum, the indirect band gap and band-to-band transition is conformed for both compounds. Moreover, these compounds absorb light within 5 to 25 eV incident photon energy. Hence, these materials are good light absorbers; therefore, they can be used in optoelectronic devices.

Author Contributions: All authors contributed equally in the article in conceptualization, methodology, investigation, analysis, validation, writing original draft, review and editing. All authors have read and agreed to the published version of the manuscript.

Funding: Deanship of Scientific Research at King Khalid University Abha 61421, Asir, Kingdom of Saudi Arabia through the Large Groups Project under grant number RGP.2/225/43 and Taif University Researchers Supporting Project Number (TURSP-2020/349), Taif University, Taif, Kingdom of Saudi Arabia.

Data Availability Statement: There is no data to disclose.

Acknowledgments: The authors extend their appreciation to the Deanship of Scientific Research at King Khalid University Abha 61421, Asir, Kingdom of Saudi Arabia for funding this work through the Large Groups Project under grant number RGP.2/225/43. The research was supported by the Taif University Researchers Supporting Project Number (TURSP-2020/349), Taif University, Taif, Kingdom of Saudi Arabia.

Conflicts of Interest: There is no conflict of interest to declare.

References

1. Sukhatme, S.P.; Nayak, J.K. *Solar Energy*; McGraw-Hill Education: New York, NY, USA, 2017; ISBN 9352607120.
2. Asafu-Adjaye, J. The relationship between energy consumption, energy prices and economic growth: Time series evidence from Asian developing countries. *Energy Econ.* **2000**, *22*, 615–625. [CrossRef]
3. Rodríguez Cervantes, F.J. Optimización de un Secador Solar Basado en el Método de Análisis Exergético. Ph.D. Thesis, Universidad de Ciencias y Artes de Chiapas, Tuxtla Gutiérrez, Mexico, 2016.
4. Sharma, S.; Jain, K.K.; Sharma, A. Solar cells: In research and applications—A review. *Mater. Sci. Appl.* **2015**, *6*, 1145. [CrossRef]
5. Goodenough, J.B.; Park, K.-S. The Li-ion rechargeable battery: A perspective. *J. Am. Chem. Soc.* **2013**, *135*, 1167–1176. [CrossRef] [PubMed]
6. Stranks, S.D.; Eperon, G.E.; Grancini, G.; Menelaou, C.; Alcocer, M.J.P.; Leijtens, T.; Herz, L.M.; Petrozza, A.; Snaith, H.J. Electron-Hole Diffusion Lengths Exceeding 1 Micrometer in an Organometal Trihalide Perovskite Absorber. *Science* **2013**, *342*, 341–344. [CrossRef]
7. Rose, G. *De Novis Quibusdam Fossilibus Quae in Montibus Uraliis Inveniuntur*; Typis AG Schadii: Berlin, Germany, 1839.
8. Husain, M.; Rahman, N.; Albalawi, H.; Ezzine, S.; Amami, M.; Zaman, T.; Rehman, A.U.; Sohail, M.; Khan, R.; Khan, A.A. Examining computationally the structural, elastic, optical, and electronic properties of CaQCl 3 (Q = Li and K) chloroperovskites using DFT framework. *RSC Adv.* **2022**, *12*, 32338–32349. [CrossRef] [PubMed]
9. Zhu, Y.; Poddar, S.; Shu, L.; Fu, Y.; Fan, Z. Recent progress on interface engineering for high-performance, stable perovskites solar cells. *Adv. Mater. Interfaces* **2020**, *7*, 2000118. [CrossRef]
10. Kojima, A.; Teshima, K.; Shirai, Y.; Miyasaka, T. Organometal halide perovskites as visible-light sensitizers for photovoltaic cells. *J. Am. Chem. Soc.* **2009**, *131*, 6050–6051. [CrossRef]
11. Ayaz, U.; Shazia; Abdullah; Husain, M.; Rahman, N.; Bonyah, E. Ab initio investigation of structural, electronic, magnetic, elastic, and optical properties of Cs-based chloro-perovskites $CsXCl_3$ (X = Be and Rh). *AIP Adv.* **2021**, *11*, 105215. [CrossRef]
12. Cherrad, D.; Maouche, M.; Maamache, M.; Krache, L. Influence of valence electron concentration on elastic, electronic and optical properties of the alkaline-earth tin oxides A3SnO (A = Ca, Sr and Ba): A comparative study with ASnO3 compounds. *Phys. B Condens. Matter* **2011**, *406*, 2714–2722. [CrossRef]
13. Murad, K.; Murtaza, G.; Noman, M.; Khan, S. To study the structural, electronic and optical properties of predicted stable halide perovskites ABX3. *arXiv* **2021**, arXiv:2102.11577.
14. Gómez–Peralta, J.I.; Bokhimi, X. Discovering new perovskites with artificial intelligence. *J. Solid State Chem.* **2020**, *285*, 121253. [CrossRef]
15. Blaha, P.; Schwarz, K.; Madsen, G.K.H.; Kvasnicka, D.; Luitz, J. *wien2k. An Augmented Plane Wave Plus Local Orbitals Program for Calculating Crystal Properties*; Vienna University of Technology: Vienna, Austria, 2001; Volume 60.
16. Vujović, M.; Ragavendran, V.; Arsić, B.; Kostić, E.; Mladenović, M. DFT calculations as an efficient tool for prediction of Raman and infra-red spectra and activities of newly synthesized cathinones. *Open Chem.* **2020**, *18*, 185–195. [CrossRef]
17. Laurent, A.D.; Jacquemin, D. TD-DFT benchmarks: A review. *Int. J. Quantum Chem.* **2013**, *113*, 2019–2039. [CrossRef]
18. Singh, D.J.; Nordstrom, L. *Planewaves, Pseudopotentials, and the LAPW Method*; Springer Science & Business Media: Berlin, Germany, 2006; ISBN 0387296840.
19. Blaha, P.; Schwarz, K.; Tran, F.; Laskowski, R.; Madsen, G.K.H.; Marks, L.D. WIEN2k: An APW+ lo program for calculating the properties of solids. *J. Chem. Phys.* **2020**, *152*, 74101. [CrossRef]
20. Medvedev, M.G.; Bushmarinov, I.S.; Sun, J.; Perdew, J.P.; Lyssenko, K.A. Density functional theory is straying from the path toward the exact functional. *Science* **2017**, *355*, 49–52. [CrossRef] [PubMed]
21. Jiang, H. Band gaps from the Tran-Blaha modified Becke-Johnson approach: A systematic investigation. *J. Chem. Phys.* **2013**, *138*, 134115. [CrossRef] [PubMed]
22. Murnaghan, F.D. The compressibility of media under extreme pressures. *Proc. Natl. Acad. Sci. USA* **1944**, *30*, 244. [CrossRef]
23. Koller, D.; Tran, F.; Blaha, P. Improving the modified Becke-Johnson exchange potential. *Phys. Rev. B* **2012**, *85*, 155109. [CrossRef]
24. Khan, S.; Zaman, S.U.; Ahmad, R.; Mehmood, N.; Arif, M.; Kim, H.J. Ab initio investigations of structural, elastic, electronic and optical properties of the fluoroperovskite TIXF3 (X = Ca, Cd, Hg, and Mg) compounds. *Mater. Res. Express* **2020**, *6*, 125923. [CrossRef]
25. Ambrosch-Draxl, C.; Sofo, J.O. Linear optical properties of solids within the full-potential linearized augmented planewave method. *Comput. Phys. Commun.* **2006**, *175*, 1–14. [CrossRef]
26. Berri, S.; Ibrir, M.; Maouche, D.; Attallah, M. Robust half-metallic ferromagnet of quaternary Heusler compounds ZrCoTiZ (Z = Si, Ge, Ga and Al). *Comput. Condens. Matter* **2014**, *1*, 26–31. [CrossRef]
27. Kieslich, G.; Sun, S.; Cheetham, A.K. An extended tolerance factor approach for organic–inorganic perovskites. *Chem. Sci.* **2015**, *6*, 3430–3433. [CrossRef]
28. Rahman, N.; Husain, M.; Yang, J.; Murtaza, G.; Sajjad, M.; Habib, A.; Karim, A.; Haq, M.U.; Rauf, A.; Nisar, M. First Principle Study of Structural, Electronic, Elastic, and Magnetic Properties of Half-Heusler Compounds ScTiX (X = Si, Ge, Pb, In, Sb, and Tl). *J. Supercond. Nov. Magn.* **2020**, *33*, 3915–3922. [CrossRef]
29. Yu, R.; Zhang, X.F.; De Jonghe, L.C.; Ritchie, R.O. Elastic constants and tensile properties of Al 2 OC by density functional calculations. *Phys. Rev. B* **2007**, *75*, 104114. [CrossRef]

30. Łepkowski, S.P.; Gorczyca, I. Ab initio study of elastic constants in In x Ga 1−x N and In x Al 1−x N wurtzite alloys. *Phys. Rev. B* **2011**, *83*, 203201. [CrossRef]
31. Jamal, M.; Bilal, M.; Ahmad, I.; Jalali-Asadabadi, S. IRelast package. *J. Alloys Compd.* **2018**, *735*, 569–579. [CrossRef]
32. Grimvall, G. *Thermophysical Properties of Materials*; Elsevier: Amsterdam, The Netherlands, 1999; ISBN 0080542867.
33. Pugh, S.F. XCII. Relations between the elastic moduli and the plastic properties of polycrystalline pure metals. *Lond. Edinb. Dublin Philos. Mag. J. Sci.* **1954**, *45*, 823–843. [CrossRef]
34. Mott, P.H.; Dorgan, J.R.; Roland, C.M. The bulk modulus and Poisson's ratio of "incompressible" materials. *J. Sound Vib.* **2008**, *312*, 572–575. [CrossRef]
35. Wachter, P.; Filzmoser, M.; Rebizant, J. Electronic and elastic properties of the light actinide tellurides. *Phys. B Condens. Matter* **2001**, *293*, 199–223. [CrossRef]
36. Pettifor, D.G. Theoretical predictions of structure and related properties of intermetallics. *Mater. Sci. Technol.* **1992**, *8*, 345–349. [CrossRef]
37. Pathak, A.K.; Vazhappilly, T. Ab initio study on structure, elastic, and mechanical properties of lanthanide sesquioxides. *Phys. Status Solidi* **2018**, *255*, 1700668. [CrossRef]
38. Zener, C. Interaction between the d-shells in the transition metals. II. Ferromagnetic compounds of manganese with perovskite structure. *Phys. Rev.* **1951**, *82*, 403. [CrossRef]
39. Mayer, B.; Anton, H.; Bott, E.; Methfessel, M.; Sticht, J.; Harris, J.; Schmidt, P.C. Ab-initio calculation of the elastic constants and thermal expansion coefficients of Laves phases. *Intermetallics* **2003**, *11*, 23–32. [CrossRef]
40. Adler, S.L. Quantum theory of the dielectric constant in real solids. *Phys. Rev.* **1962**, *126*, 413. [CrossRef]
41. Smith, N. V Photoelectron energy spectra and the band structures of the noble metals. *Phys. Rev. B* **1971**, *3*, 1862. [CrossRef]
42. Kramers, H.A. La diffusion de la lumiere par les atomes. *Atti Cong. Intern. Fisica Como* **1927**, *2*, 545–557.
43. Kronig, R.d.L. On the theory of dispersion of X-rays. *Josa* **1926**, *12*, 547–557. [CrossRef]